DIPSI Workshop 2011 on Droplet Impact Phenomena & Spray Investigation
May 27, 2011, Bergamo, Italy

CAVITATION INSIDE ENLARGED AND REAL-SIZE FULLY TRANSPARENT INJECTOR NOZZLES AND ITS EFFECT ON NEAR NOZZLE SPRAY FORMATION

N. Mitroglou, M. Gavaises*, J.M. Nouri and C. Arcoumanis

Energy and Transport Research Centre
School of Engineering and Mathematical Sciences, City University London, UK
*corresponding author email: m.gavaises@city.ac.uk

ABSTRACT
The effect of string cavitation in various transparent Diesel injector nozzles on near nozzle spray dispersion angle is examined. Additional PDA measurements on spray characteristics produced from real-size transparent nozzle tips are presented. High-speed imaging has provided qualitative information on the existence of geometric and string cavitation, simultaneously with the temporal variation of the spray angle. Additional use of commercial and in-house developed CFD models has provided complimentary information on the local flow field. Results show that there is strong connection between string cavitation structures and spray instabilities. Moreover, elimination of string cavitation results in a stable spray shape that is only controlled by the extent of geometric-induced cavitation pockets. Finally, PDA measurements on real-size transparent nozzle tips have confirmed that such nozzles reproduce successfully the sprays generated by production metal nozzles.

INTRODUCTION

The role of the fuel injection system in modern direct-injection Diesel engines is paramount and well recognised as a means of controlling their performance and meeting the ever more stringent emission regulations. Electronic common-rail injection systems employ a variety of nozzle designs and engine optimisation injection strategies to cover a wide range of operating conditions that modern Diesel engines are expected to perform. Increasing injection pressure, piezo-controlled mechanisms for achieving fast response of the needle valve and multiple injections are among the methods explored and known to improve combustion and engine performance. However, under such operating conditions, cavitation phenomena are present inside the nozzle and become the dominant and frequently uncontrolled flow characteristics that affect fuel system durability and the properties of the near-nozzle emerging spray. Success of modern Diesel direct-injection fuel equipment is based on their ability to control accurately timing, duration, rate and number of injections, as well as, shaping of the spray pattern to match piston-bowl geometry and enhanced cyclic variability behaviour employing a number of different nozzle designs. Investigations over the years have demonstrated that Diesel injector nozzles generate cavitation [1-3] under typical operating conditions, a fact that complicates further the already complex design of high-pressure Diesel injection systems. As demonstrated in [4-6], two distinct forms of cavitation have been identified inside injection nozzles, geometrically-induced and vortex or string cavitation. Geometric-induced cavitation is the most common form of cavitation and it has become gradually a well-understood phenomenon; it initiates at sharp hole inlet corners due to the abrupt acceleration of the fuel flow as it enters the nozzle holes. This increase of velocity creates a pressure drop which induces cavitation at the core of the recirculation zone formed at the hole inlet; this is more pronounced with sharper rather than rounded inlet hole geometries achieved through hydro-grinding. On the other hand, string or vortex cavitation structures have been observed in the bulk of the liquid inside sac, mini-sac and valve covering orifice (VCO) nozzles, where the formed internal volume allows for formation of relatively large-scale vortical structures [7-9]. Vortex cavitation is commonly found in propellers, hydraulic turbines and hydrofoils as explained in [10-13] However, recent studies have confirmed similar behaviour in multi-hole nozzles for high-pressure direct-injection gasoline engines and low-speed two-stroke Diesel engines [7, 14-17].

Cavitation is linked to undesirable effects such as sharp reduction in engine performance, increase in noise and vibrations, as well as surface erosion [15]. In most cases of practical interest, cavitation bubbles survive until the nozzle hole exit [4]. Therefore, it is generally accepted that cavitation promotes fuel atomisation, which is desirable for enhanced air fuel mixing. However, some studies [18] have indicated that cavitation may also be associated with hole-to-hole and cycle-to-cycle variations. Appropriate design of the inlet hole curvature and the non-cylindrical shape of the holes as [19, 20] showed, alter cavitation inception and development characteristics; at the same time, careful system optimisation is found to achieve reduction of engine exhaust emissions while maintaining similar performance standards [7, 15]. Until recently, different cavitation regimes have been addressed independently. However, there is evidence [5] that geometric-induced and vortex cavitation possibly interact in various ways. Additionally, recent investigations have concluded that inception of string cavitation is dramatically enhanced and owes its existence to sources of vapour already present inside the nozzle volume [8]. These latest findings indicate that interaction of co-existing different cavitation structures possibly require further investigation, particularly at low and intermediate needle valve lifts where, needle-seat cavitation may also exist.

Experimental investigations for obtaining real-time in-nozzle flow measurements in production FIE systems, during an injection event, are rendered difficult and, in most cases, impossible to be conducted. Therefore, majority of the reported experimental studies involve configurations simulating Diesel engine operating conditions. A number of investigations have examined the development of cavitation in transparent large-scale nozzle replicas, as presented in [21-24]. A limited number of studies have also demonstrated dynamic flow similarity based on, simultaneous, matching of Reynolds and cavitation numbers. The latter allows for comparison between the two-phase flow regimes formed inside real-size and enlarged nozzles of identical scaled-up geometric characteristics [3, 25]. Simulations reported for real-size and scaled-up models using a variety of cavitation models [26] have confirmed that similar flow regimes are formed despite obvious differences in the micro-scale level of bubble formation and development The latter is effectively the effect of a large number of cavitation bubbles that coalesce and form the macroscopically observed cavitation cloud.

Following the well-established large-scale, steady-state nozzle flow studies, significant effort has been made towards manufacturing of real-size transparent nozzles. The motivation and driving force behind these efforts is summarised in the need to confirm the existence of the afore-mentioned cavitation structures and to gain insight of the highly transient flow developing during an injection event. Until recently, the majority of manufactured real-size nozzles have been simplified single-hole geometries that generally confirm the presence of geometric-induced cavitation [2, 27]. The research group at City University London were the first to substitute one of the holes of a production nozzle with a quartz window of identical geometric characteristics; an experimental breakthrough that provided valuable information on flow and cavitation structures inside a real-size multi-hole injector under realistic operating conditions [3, 28, 29]. A step forward is realised in [19], where a 3-hole, real-size, fully transparent Diesel nozzle is presented and optical access inside the sac volume is also granted.

The advances in internal nozzle flow studies under fully transient and realistic operating conditions have provided valuable information and validation data for CFD cavitation models capable of predicting the various forms of cavitation; for example see [30-32]. Experimental validation of numerical CFD models is rendered essential and supplementary to understanding the flow processes in complicated nozzle geometries and ultimately, to the design of new nozzle designs. However, the difficulty associated to manufacturing of real-size, transparent nozzles that are exact replicas of real nozzle geometries impose simplifications to the design of the nozzle itself and the transient operation of the needle. Moreover, complications related to the physical properties and the quality of the working fluids imposes additional difficulties. Furthermore, the scarce data available in real-size transparent nozzles are limited to pressures an order of magnitude lower than those currently used in modern Diesel engines. Increase of the injection pressure beyond 2000bar in the forthcoming future [33] is expected to affect fuel properties and thus, cavitation, as recently reported in [34]. More importantly, highly transient flow dynamics caused by fast needle response times give rise to the formation of vortical structures and therefore, to string cavitation [8]. Transient effects have also been correlated to increased probability of surface erosion damage [35], which is attributed to both, hole and string cavitation. Nevertheless, combination of experimental data obtained in both, large-scale and real-size injector nozzles are considered valuable for the development and validation of cavitation models applicable for fuel injectors.

The present paper represents a continuation of the work presented recently in [8, 17, 36]. Main investigations focus on the effect of string cavitation in various Diesel injectors on near nozzle spray dispersion angle both, in large-scale and real-size transparent nozzle tips. Near nozzle spray vicinity is defined at a distance of about one injection hole length downstream the nozzle exit plane. Acquired data and thorough investigations are based on a number of fully transparent nozzle replicas, as well as, real-size nozzle tips that provide unobstructed optical access of the nozzle sac volume, injection holes and sprays formed at the nozzle exit. Image collection over sufficient duration periods, for steady-state experiments and adequate imagining frame rates, for transient operating conditions, have provided qualitative information on the existence of geometric and string cavitation, simultaneously with the temporal variation of the spray angle. Investigated designs include 6-hole nozzle configurations of valve-covering orifice (VCO), mini-sac, as well as a new prototype nozzle design that promises to eliminate string cavitation and produce steady spray shapes. Simultaneous use of two synchronised high-speed cameras allowed for visualisation of all forms of cavitation inside the nozzle volume, as a function of needle lift and operating condition. At the same time, use of commercial and in-house developed CFD models has provided complimentary information on the local flow field of the tested nozzles. Finally, assessment of real-size transparent nozzle tips is achieved in terms of emerging spray characterisation through the use of PDA measurements. The latter aims to demonstrate that such real-size transparent nozzle tips reproduce adequately the internal flow and spray characteristics of real-size metal nozzles. Then the various results obtained are presented while the most important findings are summarised at the end.

EXPERIMENTAL SET-UP

Presented results in following sections have been obtained in both, enlarged and real-size transparent nozzle models. Figure 1 illustrates the two basic nozzles where studies are based on. An additional nozzle design is used for the large-scale experimental and computational cases.

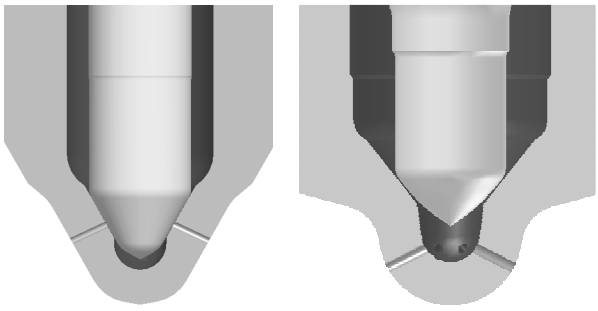

Figure 1: Investigated nozzle geometries. (a) valve-covering orifice (VCO) and (b) sac type nozzles with a 6-hole configuration.

The main characteristics of its configuration include elimination of sac volume and independent flow path for all six injection holes; as a result, flow interconnection among the holes is eliminated. All transparent nozzles (large-scale and

real-size) were manufactured from a clear, acrylic material. The scaling factor of the enlarged models was chosen to be ten (x10) times the real-size nozzle. All nozzles share injection holes of cylindrical shape. All designs feature sharp hole entries, and their diameters vary from 136×10^{-6} m to 300×10^{-6} m in real-size dimensions. The large variation in injection holes diameters among all nozzles is attributed to their field of operation; low diameter values represent nozzles that operate in engines fitted on passenger vehicles, while large injection hole diameters refer to injectors for large power production units installed on land or on marine applications. In the following sections the experimental set-up for both large-scale and real-size investigations is presented.

Enlarged Model Test-Rig

A schematic overview of the experimental setup with the incorporated large-scale model is shown in Figure 2. Two different variations of this rig have been utilised; the first one is a closed-loop flow circuit and injection takes places in to liquid. Dynamic flow similarity to realistic operating conditions is achieved based on Reynolds and cavitation numbers. Such flow similarity assists in interpretation of cavitation flow regimes formed inside the transparent nozzle relative to a real-size case. The second variation incorporates injection against atmospheric quiescent environment exhibiting open-loop circuit (variation presented in Figure 2).

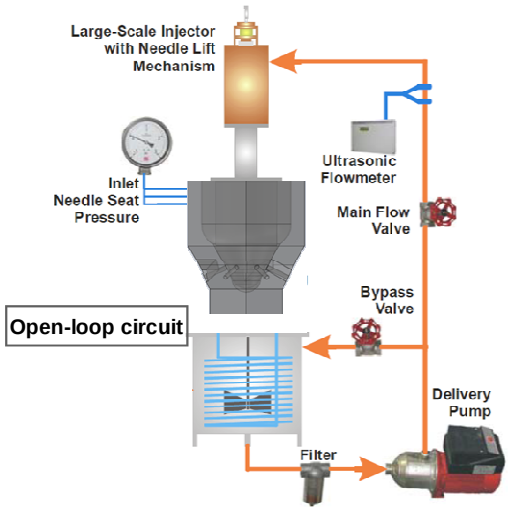

Figure 2: Schematic of the enlarged model test-rig. The open-air injection variation is presented.

The latter has proven to be a promising solution to simultaneous visualisation of in-hole cavitation structures and emerging spray shape. The present system is not expected to represent exact flow fields encountered in a real injection event. Firstly, it is a steady-state experiment, thus it does not account for transient needle movement. Moreover, realistic flow conditions cannot be matched, therefore, dynamic flow similarity to real-size flow fields assists in gaining physical understanding of the specific nozzle flow characteristics and validation of simulation results. Additionally, acquired information is rendered useful, as it is explained in following sections, since it allows for internal nozzle flow structures to be linked to the near nozzle spray stability.

The flow rate through the nozzle is controlled by a valve fitted downstream the liquid delivery pump and measured by an ultrasonic flow meter. In the case of injection in to liquid (closed-loop variation of the rig), simulation of sub-atmospheric chamber pressure conditions and therefore, high cavitation numbers, is achieved by a suction pump. The latter is installed on the drain side of the circuit. Reynolds number is defined on the basis of mean flow rate through the nozzle and average hole diameter, while the definition of cavitation number is as follows in Eq. (1):

$$CN = \frac{\left(P_{inj} - P_{back}\right)}{\left(P_{back} - P_{vapour}\right)} \quad (1)$$

The working fluid is water and its temperature is kept constant at 25°C.

Flow through a multi-hole nozzle, and especially through the injection holes, is known to be highly turbulent. Although the experiment was run under steady-state conditions, all flow features and, in particular, cavitation structures, are expected to behave transiently and to exhibit short time scales. This dynamic behaviour is captured by an advanced high-speed digital imaging technique at frame rates varying from 20k – 50k frames per second.

Real-Size Transparent Tip Test-Rig

Investigations of internal flow and cavitation formation inside a real-size nozzle operating under highly transient realistic conditions are achieved by replacement of the nozzle tip with an exact replica transparent cap. The technique has been developed and presented thoroughly in [36, 37]. A brief description of the required modifications is illustrated in Figure 3. Finally, the clamping mechanism of the transparent tip on to the metallic nozzle body is shown in Figure 4.

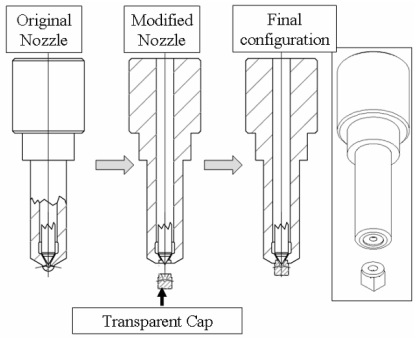

Figure 3: Nozzle modifications and transparent tip assembly [36].

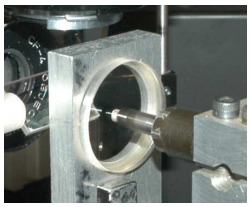

Figure 4: Clamping mechanism of transparent nozzle tip.

The experimental set-up used to capture the effect of cavitation on the emerging fuel spray involved a dual, high-speed imaging technique. First, high-speed imaging provided information on the onset and development of cavitation inside the injection hole, while, at the same time, the emerging fuel spray was captured on a second high-speed camera that was focused on the first 2mm downstream of the exit of the

injection hole. As illustrated in the set-up schematic in Figure 5, the real-size dimensions of the nozzle did not allow for the two cameras to lie on the same horizontal plane, thus necessitating a complex setup utilising a 50-50 wideband beam splitter that allowed one camera to access the in-hole flow through the beam splitter and the second to utilise the built-in mirror feature of the splitter on the vertical plane. The selected light source for best possible illumination was a high-power (~20W) pulsed laser. An advantage of the selected illumination source was the pulse width of the laser used, as it determines the image exposure duration, and it was of the order of 150-180 ns; an exposure duration that cannot be matched by any high-speed camera available. The drawback in that system has been its inability to perform at pulse frequencies greater than 6 KHz. The latter has limited the maximum possible imaging frame rate to 6000 frames per second.

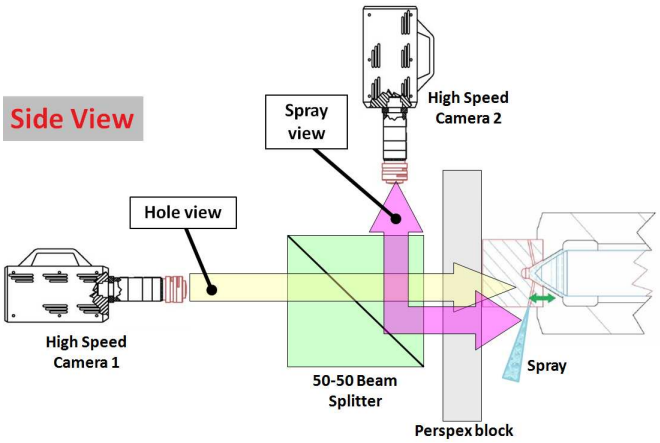

Figure 5: Dual imaging set-up schematic.

Detailed phase–Doppler anemometry (PDA) measurements completed the real-size, transparent nozzle tip experiments. The PDA system setup chosen for this investigation is illustrated in Figure 6. The system is a 2-dimensional PDA system where the vertical (u) and horizontal (v) velocity components are measured simultaneously for each droplet. PDA is a point measurement technique and selection of the measurement plane and grid are essential. It is well accepted that the closer the measured points to the nozzle exit are, the better the understanding of the nozzle performance; however, given the high injection pressures of Diesel nozzles (above 300bar is considered to be a high injection pressure for this type of measurement), fuel jets tend to have a significantly dense liquid core as soon as they exit the nozzle which renders impossible any attempts to measure within that region. This is mainly due to attenuation of the laser beam when it penetrates high-pressure dense sprays with a pronounced liquid core. The compromise that is often made is to move the measurement plane further away from the nozzle exit. In the present experiment, the measurements plane was set at 10 mm away from the nozzle exit, where higher data rates were achieved and a smaller number of injections was needed, as transparent nozzle tips are replaced after approximately 100 injection events. The latter is a necessity due to certain wear that appears in the acrylic tips caused by high-pressure fuel flow.

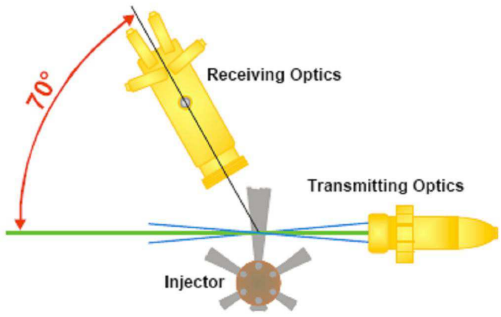

Figure 6: Optical configuration of the phase – Doppler anemometer (PDA) system.

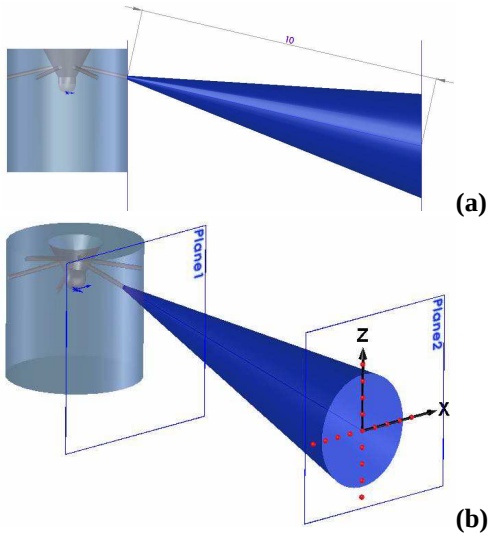

Figure 7: Schematic representation of the PDA measurements grid; (a) axial plane distance from nozzle exit and (b) grid points definition.

Figure 7 schematically illustrates the location, in space, of the measurement plane and grid relative to the injection hole exit. Points, where data were acquired, lie on two normal axes as shown by red dots in Figure 7(b). The spatial resolution of the above grid is 0.5mm.

RESULTS AND DISCUSSION

In this section the various results will be presented and discussed. Initially, the results obtained from the combined investigation of internal nozzle flow and emerging spray of a valve-covering orifice (VCO) nozzle are presented. Those include images of in-hole cavitation structures, focused particularly on string cavitation, as well as the emerging spray shape for several operating conditions including various needle lifts, Reynolds and cavitation numbers. Following the VCO large-scale study, results from a prototype nozzle design are presented. This design promises to eliminate string cavitation inside the injection holes, thus, it exhibits stable sprays under all tested operating conditions. Internal nozzle flow results accompanied by spray images are presented. Finally, spray characterisation results from a real-size transparent tip VCO nozzle are presented. These results include particle velocity and size measurements conducted at sprays produced by a transparent tip converted VCO nozzle.

Large-Scale VCO Nozzle Study

The study of the VCO nozzle geometry includes various operating conditions: low and full needle lift cases, low and high cavitation numbers, as well as a variety of flow rates through the nozzle are included. The manufactured large-scale VCO nozzle replica is ten times (×10) larger than the real-size nozzle and it features sharp hole inlet. The latter is important since a fair amount of geometric-induced cavitation is present inside the injection hole; consequently, nozzle discharge coefficient varies from 0.26, at lowest needle lift, to 0.47 at maximum needle lift. Additionally, cavitation and Reynolds numbers of all tested conditions vary from 3 to 6.5 and 12 000 to 27 500, respectively.

The first observation is done at 20×10^{-6} m needle lift, cavitation number of 3 and low Reynolds number, of the order of 12 000. At such low flow rate conditions geometric – induced cavitation is minimum inside the hole (Figure 8); therefore, emerging spray is not atomised. Moreover, it is clearly seen on the sequence of images presented in Figure 8 that string cavitation has been observed. Its presence is not continuous, it is rather switching on and off during the tests. Additionally, it is found to have a profound effect on the spray cone angle. The mechanism of string formation under these low flow rate conditions has confirmed and is in full agreement with observations presented in [17]. According to what has been recorded, vapour visualised as a 'string' is not actually 'cavitation' but air entering into the nozzle from the hole exit. Swirling flow patterns inside the injection hole possibly cause sufficient pressure drop allowing for air from outside the nozzle to enter the injection hole and travel upstream towards the sac volume. Once this stream of air reaches the hole inlet, it interacts instantly with geometric-induced cavitation at that location. Therefore, cavitation pockets are generated at the hole inlet due to strong interaction with the stream of air/bubbles. Following induction of geometric-induced cavitation, the flow field inside the injection hole is altered, thus, influencing spray stability. The resulting effect on spray angle has been quantified and the recorded data of string cavitation inside the nozzle hole and spray cone angle show a change of approximately 30°. Precisely, when no string is present, spray cone angle varies from 18°-20°; however, when string cavitation is observed inside the hole, spray cone angle is measured to be of the order of 50°.

Increasing Reynolds and cavitation numbers to 18000 and 6.3, respectively, flow field inside the injection hole changes marginally, at low needle lifts. Main difference is found to be on the size of the geometric – induced cavitation regime. The latter is now larger and occupies more of the cross-sectional area of the hole, as opposed to lower CN conditions, and also extends further inside the hole. As presented previously in [17, 38] the interaction between intense geometric-induced cavitation structures and string cavitation is responsible for the differentiation in spray angles of upper and lower spray boundary. In detail, when the geometric locus of the cavitation strings coincides with the area occupied by geometric-induced cavitation pockets, then the effect of the string on the spray shape is marginal. On the contrary, when string cavitation lies on the part of the hole that is not occupied by geometric cavitation then the effect on the spray shape is well pronounced; the latter is illustrated in Figure 9 by comparison of spray images against predictions of vapour in VCO nozzles.

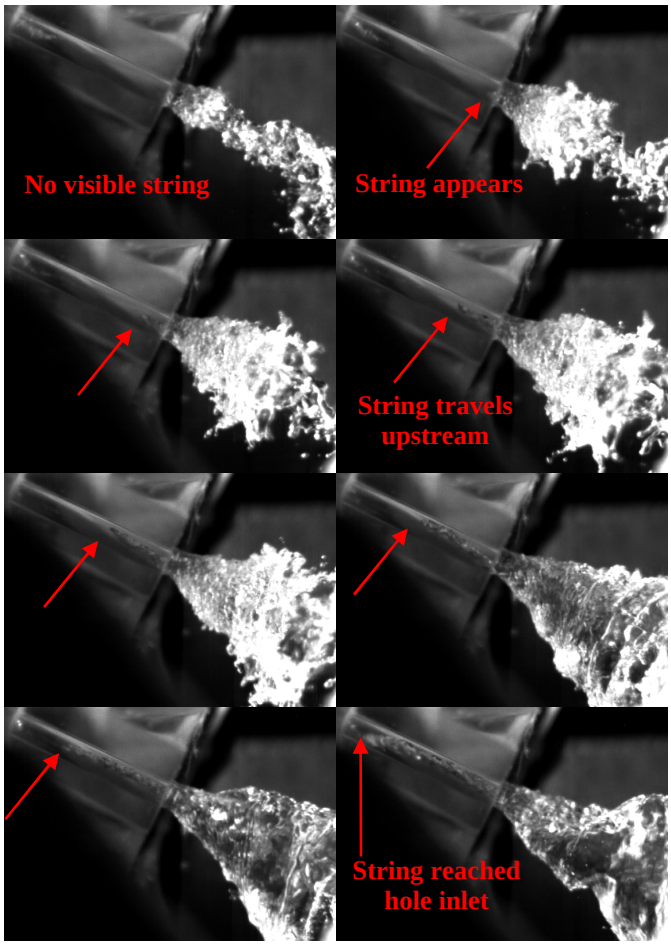

Figure 8: Developmnt of string cavitation and spray shape at 20μm needle lift, CN=3 and Re=12 000.

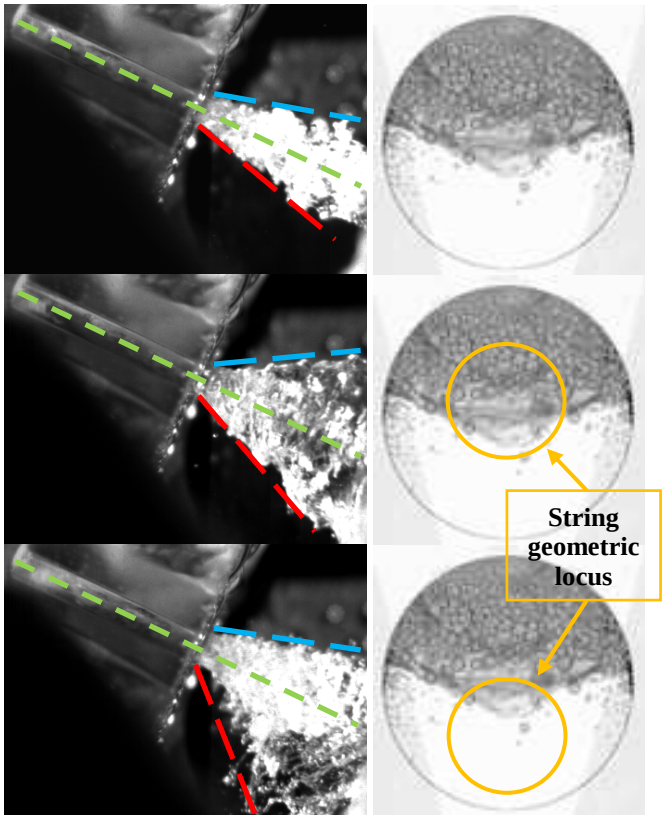

(a) (b)

Figure 9: (a) Spray shape variation images and (b) vapour distribution prediction [38]

Similar behaviour has been observed at high valve lift cases. Precisely, at full needle lift that is set to 250×10^{-6} m, geometric-induced cavitation is very intense and reaches the exit of the injection hole. Therefore, string cavitation seems to affect mainly the lower boundary of the spray as illustrated in Figure 10. Quantitatively the effect on the lower spray boundary presented in Figure 10 is reduced to 50%, as compared to the low needle lift cases (see Figure 9). The reason for this reduction lies on the fact that at high needle lift cases, the upper part of the hole is solidly occupied by geometric cavitation structures that, at high flow rates, extend to the hole exit thus, increasing atomisation. Additionally, at such high flow velocities (calculated to be larger than 15 m/s for the large-scale model), string cavitation structures rarely initiate at the hole exit and travel upstream inside the injection hole. Instead, strings are created at the core of recirculation zones forming inside the nozzle's sac volume [8]. In the case of VCO nozzles, where the sac volume is absent, a minor volume that forms between the needle face and hole inlet promotes swirling motion at the hole entry, due to injection holes flow field interactions. Therefore, this swirling motion gives rise to string structures and due to their origin location, their core consists of tiny cavitation bubbles that most probably are fed into the stream from the intense geometric cavitation structures at the hole entry and enhance its existence. Recent work by the authors in fully transparent real-size nozzles operating at pressures up to 600bar has verified that such structures can be present during real injection events.

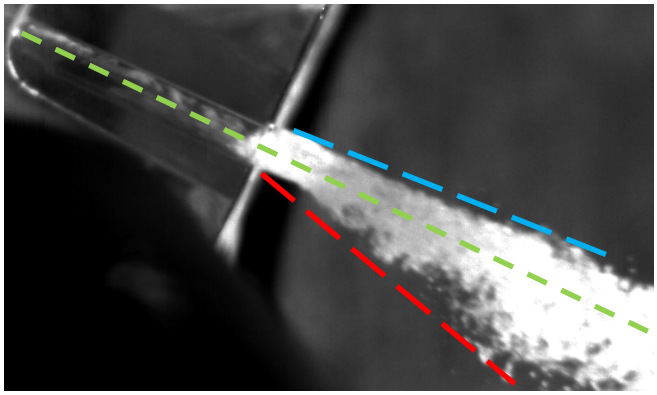

Figure 10: Observed variation in upper (blue) and lower (red) spray half angle at full needle lift and cavitation number of 6.3.

Large-Scale Prototype Nozzle Design

The authors' research group has conceived and tested a new nozzle design that eliminates the aforementioned vortex flow at the hole entry by isolating each hole's flow path. Elimination of vortex flow has been proved to affect considerably, and ultimately eliminate, vortex cavitation structures. As presented in the following Figure 11, geometric cavitation structures formed at the hole inlet are "controlled"; the latter effectively means that cavitation always takes place at the same location. The penetration of the formed vapour pocket inside the nozzle hole and resulting volume fraction are carefully 'designed' with the aid of CFD by modifying basic nozzle design characteristics. The presented nozzle design exhibits no hole inlet rounding thus, cavitation structures are intense. It is illustrated in Figure 11(a, b and c) that at various needle lifts, under constant cavitation number, formed vapour clouds extend to certain length, for each case, inside the injection hole and remain at the same location without exhibiting any transient movement in terms of their length. The swirling motion reported by various researchers [5, 29, 36] inside the injection hole is absent. Therefore, string cavitation is eliminated and emerging sprays exhibit stable shape patterns, as illustrated in Figure 12. As mentioned above, by altering certain design characteristics of this new concept nozzle design cavitation is well controlled and, consequently, different spray dispersion angles are achieved (Figure 12) and exhibited spray stability is paramount under all operating conditions. Moreover, levels of spray atomisation are well controlled by the extend of geometric cavitation structures inside the injection hole.

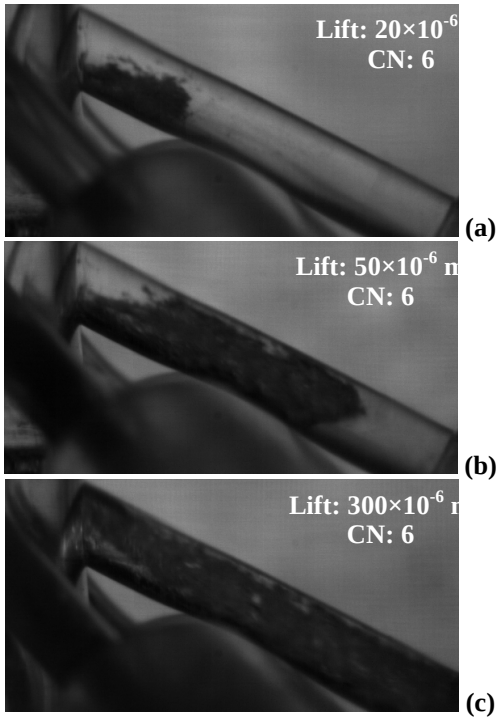

Figure 11: Cavitation imaging inside the injection hole of a new concept design nozzle at CN = 6 and (a) low needle lift of 20μm, (b) needle lift of 50μm and (c) full lift of 300μm.

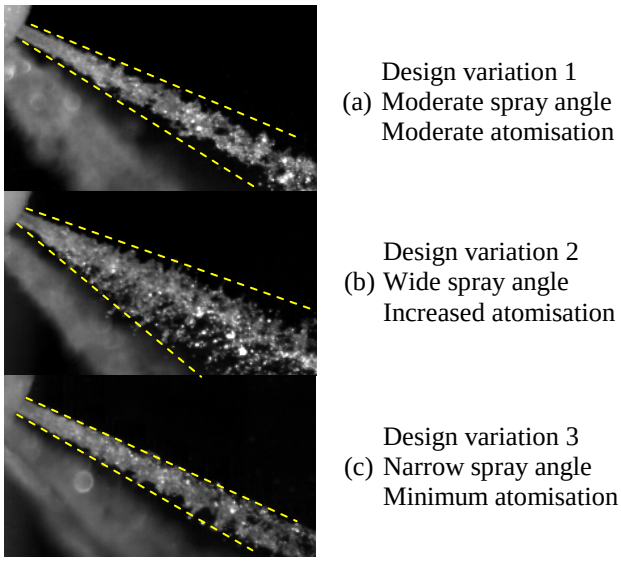

Figure 12: Spray images at steady state conditions from a new concept nozzle design for two different needle designs (a), (b) and (c).

Real-Size Transparent Nozzle Tip

Following the extensive investigations of internal flow and its effects on emerging spray shape stability in enlarged, transparent nozzle replicas, the need to confirm the existence of the observed structures in real-size nozzles has become a necessity. A selected, generic VCO nozzle has been converted to accommodate a transparent nozzle tip that allows for direct optical access inside the nozzle and injection holes. Simultaneous acquisition of images of the emerging spray enabled the establishment of the link between internal nozzle flow and emerging spray stability in real-size nozzles. However, due to the complexity of the real-size nozzle tip experiment, certain alterations to operating conditions had to be made; injection pressure is set to 30 MPa to prevent leakage and fast deterioration of the transparent nozzle cap and therefore, injection duration is set to 4ms to match the corresponding flow rates.

Detailed investigations on string cavitation have provided enough supporting evidence that structures observed in large-scale replicas also exist in real-size nozzles. Figure 13 illustrates sample acquired images and nozzle characteristics that are visible from this view angle. As illustrated below, the needle surface, the minor formed sac volume and side views of the injection holes are clearly visible. On the right-hand image of Figure 13, cavitation bubbles that started forming inside the injection hole are shown. Additionally, evidence of needle string cavitation is visible; needle string cavitation is effectively a string cavitation originates at the hole entrance, due to strong swirling flow, and extends on to the needle face.

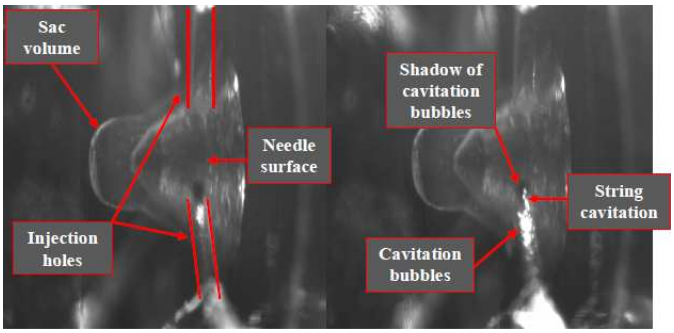

Figure 13: Sample side view images of VCO nozzle and explanation of illustrated features.

Figure 14 presents a series of images from 1.9ms – 2.5ms after triggering of injection from a 4ms injection event at 40 MPa injection pressure. It is noticed that from 2ms after triggering of injection and onwards, string cavitation appears at the hole entrance and it moves towards both directions, the needle surface and inside the hole. The latter contributes to acceleration in formation of geometric cavitation structures inside the hole. These string structures remain attached to the needle until its lift increases enough to no longer be in front of the injection holes entrance. Similar behaviour of string cavitation structures inside high-pressure injection nozzles has been verified through earlier work of the authors' research group. As injection develops, a strong swirling flow is present inside the injection hole and around its entrance. The latter enhances the formation of strings of bubbles and confirmed the previously presented behaviour of string cavitation and its formation mechanisms in the large-scale nozzle replicas.

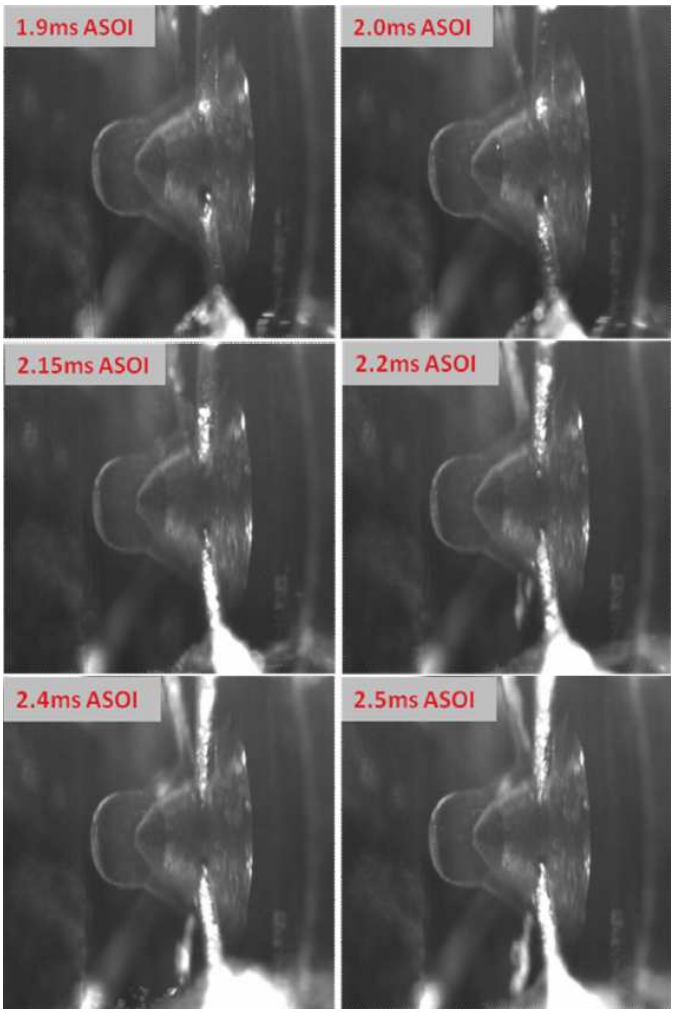

Figure 14: Time sequence of images at 300bar injection pressure and injection duration of 4ms.

Further investigations in real-size nozzles are focused to establishment of possible links between in-hole cavitation formation and development and the emerging spray structure and stability. The following dual imaging investigation includes bottom view, high-speed images of the internal hole flow and first stages of the emerging spray.

Acquired images for the standard VCO nozzle design at 40 MPa showed that at early injection stages, when cavitation has not built up inside the hole, this is immediately reflected on the emerging spray shape. Figure 15 illustrates a sequence of images for the aforementioned conditions and it can be argued that atomisation quality of the spray (right-hand side images) improves as cavitation builds up inside the hole (left-hand side images). Additionally, an extra feature that is clear from these images is that Start of Injection (SOI) happens at around 1ms after electronic triggering of the injector, which implies that the first liquid to exit the injection hole is visible at 1ms after triggering, as shown in the images below. At higher injection pressures of 40 MPa, as illustrated in Figure 16, cavitation develops faster than the lower pressure case inside the injection hole. This ensures that spray atomisation is less affected by any marginal changes of cavitation structures inside the hole. However, in Figure 16 a substantial change in spray cone angle is evident at 1.34ms after trigger. The optical set-up and lighting source used does not allow for clear interpretation of cavitation strings inside the hole, although geometric cavitation pattern does not seem to be affected from one step to the next.

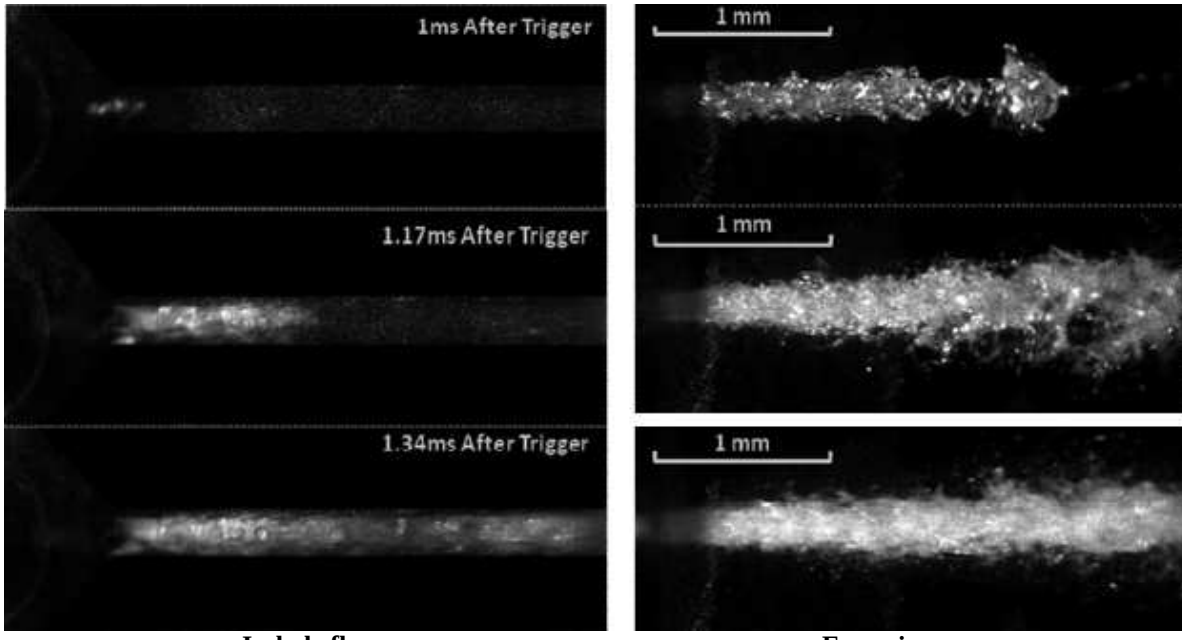

In-hole flow **Emerging spray**

Figure 15: Sequence of images at early stages of injection for the VCO nozzle design at 300bar injection pressure.

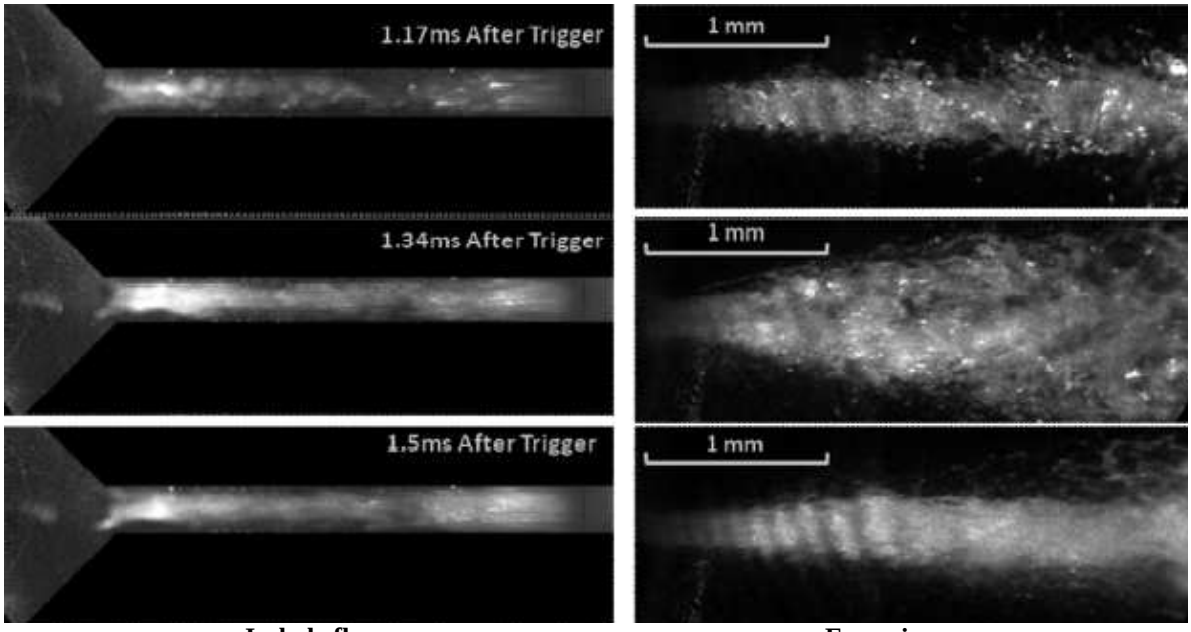

In-hole flow **Emerging spray**

Figure 16: Sequence of images from injection event at 400bar.

Finally, assessment of real-size transparent nozzle tips and complete characterisation of the spray is achieved through the use of PDA measurements. The latter aims to demonstrate that such real-size transparent nozzle tips reproduce adequately the internal flow and spray characteristics of real-size metal nozzles; additionally, it provides an extra means of quantitative measurements of spray velocities and sizes that is considered mandatory for a compete characterisation of the performance of an injector.

PDA results have been acquired for the VCO nozzle geometry, and are presented as temporal and spatial profiles. The former show the variation of the resultant velocity vector (absolute velocity and angle values are plotted) at one point for the entire injection duration. The latter show the spatial variation of the resultant velocity vectors at a certain time for more than one point at a cross section of the jet. Furthermore, droplet diameter profiles are presented in the same way. The main axis of the PDA measurement points is the vertical axis z, as shown in the top row of Figure 17(a). In the same figure, the temporal velocity profiles at three points along the vertical (z) axis are presented. The spatial resolution of the three points is 0.5mm on either sides of axis z. Droplet velocities at the centre of the jet appear to be as high as 190m/s, while from 1.5-5.5ms after triggering the velocity profile at the centre of the jet follows the behaviour of the needle lift profile. At a vertical location of 0.5mm above the centre point (z = -0.5mm), observations of unstable velocities towards the end of injection are evident. The latter is mainly attributed to intense geometric cavitation structures that transiently extend to the exit of the hole during one injection event. On the contrary, at a vertical location of 0.5mm below the centre point of the jet (Figure 17(e), z = +0.5mm), the velocity

profile and the angle of the velocity vector exhibit a stable behaviour. Figure 18 also presents temporal velocity distributions for two points at z = -1mm and z = +1mm from the centre of the jet. Velocity variations for both points follow the same trend of instabilities as previously explained, since their location is at the two edges of the jet.

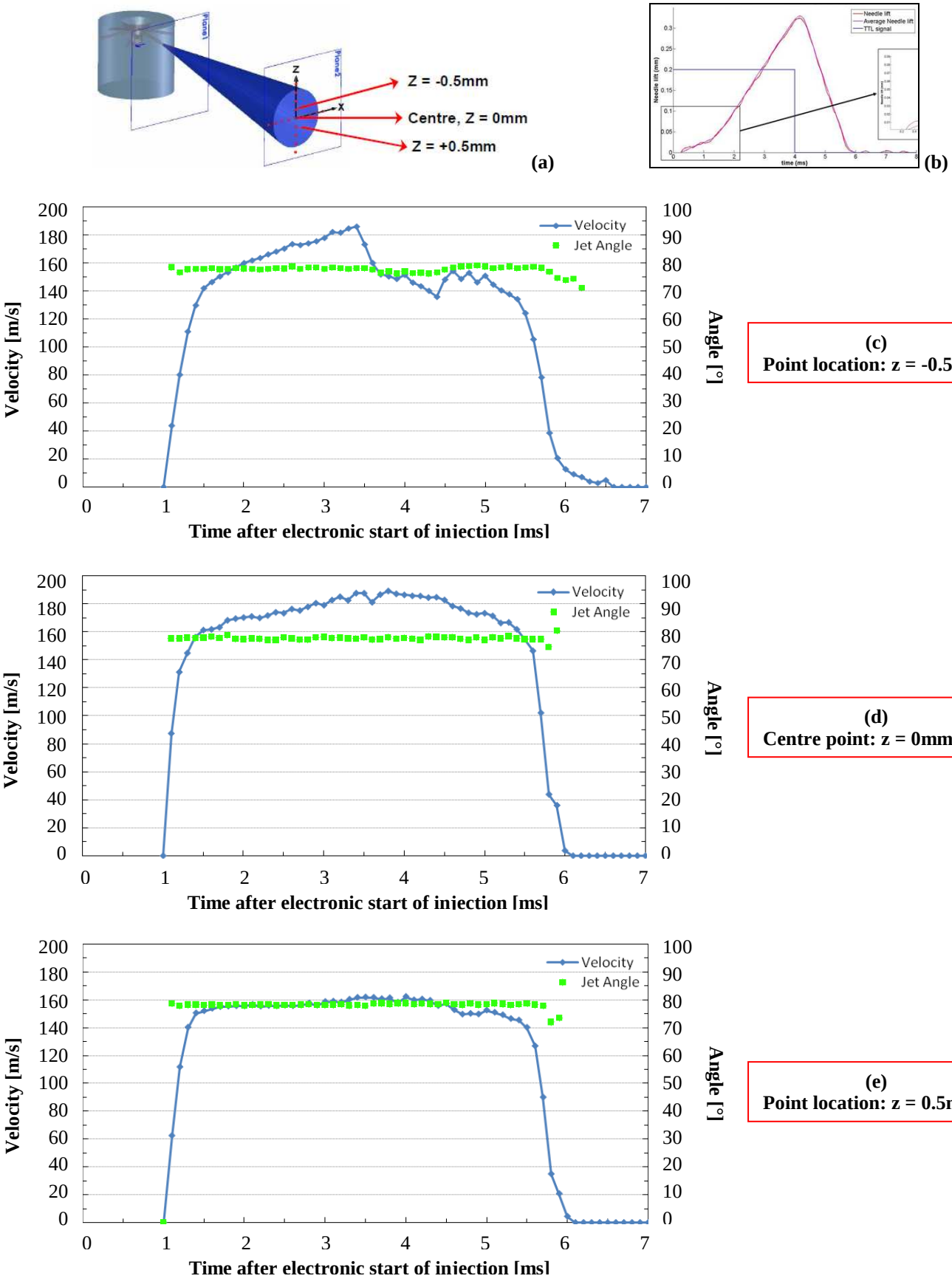

Figure 17: (a) Legend of measurements grid. (b) Needle lift profile and temporal velocity profiles at (c) z = - 0.5 mm, (d) at the centre of the jet z = 0 mm and (e) z= 0.5 mm on the z axis.

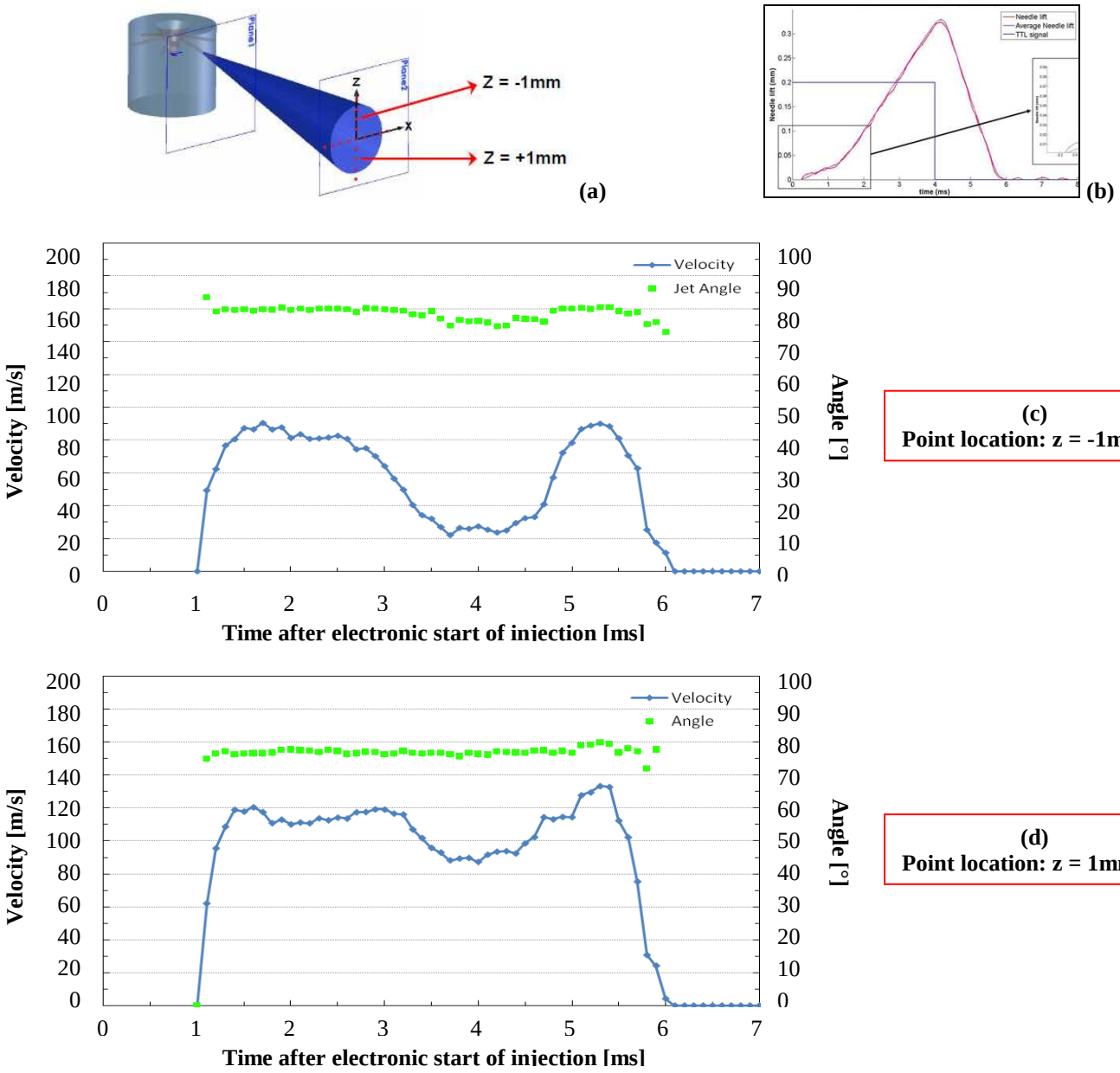

Figure 18: (a) Legend of measurements grid. (b) Needle lift profile and temporal velocity profiles at (c) z = - 1 mm and (d) z= 1 mm on the z axis.

Droplet size distribution at the centre of the VCO nozzle jet is illustrated in Figure 19, in the form of average mean (AMD) and Sauter mean diameter (SMD). Droplet sizing measurements always refer to the complete injection event and neither spatial representation at certain time steps, nor temporal variation graphs at a single point could secure a satisfactory description of the effect. Therefore, a better representation of the phenomenon is achieved, when the comparison is based on the number of droplets that crossed the measuring plane during one injection event, excluding only the tail of the spray. More specifically, judgement upon the normalised distribution graph leads to more accurate conclusions.

The graph presented in Figure 19 includes diameter values from all points measured on the vertical z axis. Although the AMD values vary slightly around the mean value of 10μm, the SMD values present a wider distribution that stabilises at values around 40μm. A rise in SMD values observed at times from 3.5 to 4 ms are directly connected to the needle closing event. The latter distribution is typical high pressure nozzle behaviour; however, it should be stressed that the tested nozzle is not a real nozzle. The transparent cap is not manufactured in a similar way to the real, all-metal, nozzle and the injection pressure is not the nominal operating pressure of production nozzles. As a result, large diameter droplets are expected to be found, contributing to the calculated high SMD values.

Droplet size data gathered from all measurement points, during the complete injection event are illustrated in Figure 20, in a normalised diameter distribution graph. The corresponding mean droplet size value is smaller than the one presented in Figure 19. The reason lies on the fact that, while the presented temporal profile corresponds to data collected during the time velocities have developed and injection has started (i.e. from 1.5 to 5 ms), the normalised diameter distribution graph takes into account the complete injection event after start of injection (i.e. from 1 to 6ms). The observed difference in mean droplet size is then directly connected to small, spherical droplets that are generated during the needle closing time and validated from the measuring system..

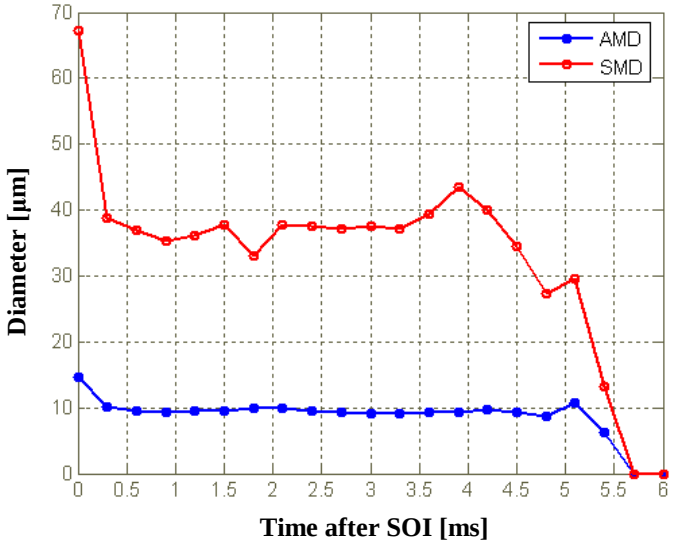

Figure 19: Temporal droplet diameter distribution at the centre of the jet (z = 0mm).

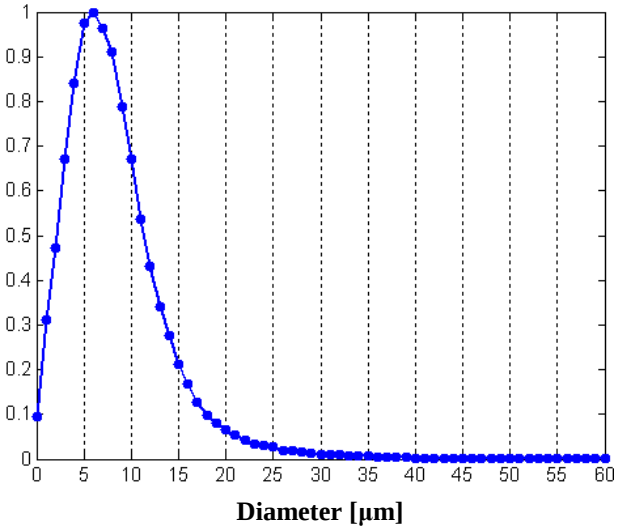

Figure 20: Normalised diameter distribution across all points of the measuring plane during the complete injection duration.

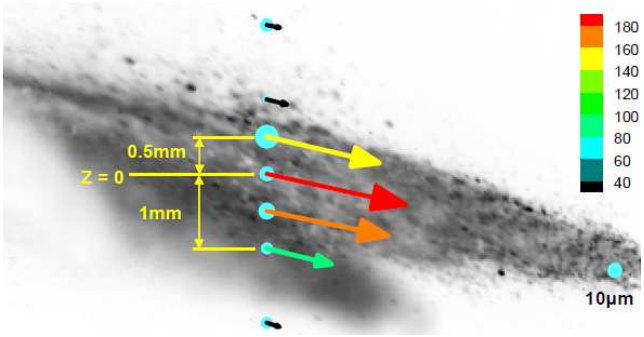

Figure 21: Spatial velocity and size profile for the VCO nozzle at 10mm along the jet axis and 4ms after triggering.

Finally, an overall representation of the measured velocities and droplet sizes across the vertical plane at 10mm along the jet axis, is given in Figure 21, where both the droplet spatial velocity and size distributions are presented; these values refer to 4ms after the triggering of injection, a time when the needle is at its maximum lift according to the previously acquired needle lift data. Moreover, in full accordance with previously presented data, the velocity profiles are those of a typical jet with the velocity values peaking around the centre axis of the jet and becoming smaller at the two edges of the jet. Additionally, the droplet sizing profiles follow the same trend as larger droplets are found at the centre of the jet, while smaller ones tend to move at its edges. Finally, the unstable behaviour of the upper half of the jet is now reflected clearly in the droplet sizing profiles; at 0.5mm above the centre point, the largest droplet diameter of the cross-section can be found.

CONCLUSIONS

Cavitation forming inside the nozzle of fuel injection equipment for Diesel engines represents the main flow feature affecting nozzle discharge coefficient, the momentum of the injected liquid and spray dispersion angle. As demonstrated in the present work, understanding of the flow mechanisms taking place inside high-pressure injection nozzles is a prerequisite for the design of advanced systems that minimise shot – to – shot variations. Moreover, the present study has provided a number of experimental data for string cavitation regarding their origin and their immediate effect on spray instabilities.

High-speed visualisation of cavitation structures forming inside enlarged and real-size VCO Diesel nozzles with cylindrical (parallel) holes has been reported. Dual imaging of cavitation structures inside the nozzle hole and the emerging spray revealed that cavitation enhances spray atomisation; increasing cavitation numbers result in the development of geometric-induced cavitation at the hole entry that, in turn, increases spray atomisation quality. Investigations also revealed and confirmed previous findings of the research group that during transient needle movement (opening and closing phases), when flow inside the hole is not fully developed, strings appear that initiate at the hole exit and travel upstream towards the entry of the hole. Presence of such string structures is found to alter the spray dispersion angle significantly and induce random instabilities. At later stages during the injection event and at times when flow is fully developed inside the hole, string cavitation is identified to initiate at the hole entry. The mechanism of creation is attributed to vortical flow structures present inside the sac volume that are generated due to hole-to-hole flow interaction. The core of these vortices interacts with the intense cavitation structures present at the hole entry, resulting to the creation of cavitation strings, whose core consists of cavitation micro-bubbles coming from already developed geometric-induced structures. Moreover, the location of cavitation strings relative to the geometric-induced cavitation inside the hole is strongly connected to the instability of upper or lower spray boundary.

Similar flow structures have been observed in real-size VCO nozzle replicas and realistic operating conditions. At injection pressures of 30 MPa, during the transient needle movement phase, string cavitation is generated at the hole entry that extends to either sides, on to the needle face, and inside the injection hole. Simultaneous imaging of the emerging spray revealed significant spray instabilities that are also attributed to unstable string cavitation structures. Geometric cavitation is found to enhance atomisation also in real-size VCO nozzles, confirming the agreement between large-scale and real-size nozzle experiments. Finally, PDA measurements on real-size transparent caps revealed that generated spray is directly comparable to that generated by

real nozzles thus, such acrylic nozzle tips consist an innovative and extremely informative means of nozzle flow investigations. Spray instabilities observed by the high-speed imaging technique have also been confirmed by the PDA measurements; unstable velocities, and spray angles have been recorded for both, upper and lower, spray boundaries.

Finally, following the understanding of various nozzle flow phenomena and the establishment of links between various forms of cavitation and spray instabilities, a new concept nozzle design has been proposed. This novel design has demonstrated stable spray angles that are directly related to certain design characteristics. The proposed nozzle hole configuration and the elimination of sac volume have diminished hole-to-hole interactions thus, eliminated vertical flow structures. The absence of string cavitation has been confirmed and the "controlled" geometric-induced cavitation demonstrated stable effects on spray dispersion angle and subsequent atomisation quality.

ACKNOWLEDGMENT

The authors would like to thank all staff members and PhD students of the Energy and Transport Research Centre of City University London that have made contributions to the cavitation research programme on Diesel injectors. Finally, the authors would like to express their gratitude to Toyota Motor Co. Japan for financial support on the real-size nozzle tip experiments.

NOMENCLATURE

VCO	Valve covering orifice	
CFD	Computational fluid dynamics	
PDA	Phase – Doppler anemometer	
SOI	Start of injection	
AMD	Arithmetic mean diameter	
SMD	Sauter mean diameter	
CN	Cavitation number	dimensionless
Re	Reynolds number	dimensionless
P_{inj}	Injection pressure	Pa
P_{back}	Chamber pressure	Pa
P_{vapour}	Vapour pressure	Pa

REFERENCES

[1] Chaves, H., M. Knapp, A. Kubitzek, F. Obermeier and T. Schneider, *Experimental study of cavitation in the nozzle hole of diesel injectors using transparent nozzles.* SAE technical paper, 1995. **950290**.

[2] Badock, C., R. Wirth, A. Fath and A. Leipertz, *Investigation of cavitation in real size diesel injection nozzles.* International journal of heat and fluid flow, 1999. **20**(5): p. 538-544.

[3] Arcoumanis, C., M. Badami, H. Flora and M. Gavaises, *Cavitation in real size multi-hole diesel injector nozzles.* Transactions Journal of Engines, SAE paper 2000-01-1249, SAE Transactions, 2000. **109**(3): p. 1485-1500.

[4] Arcoumanis, C., M. Gavaises, J.M. Nouri, E. Abdul-Wahab and R. Horrocks, *Analysis of the flow in the nozzle of a vertical multi-hole diesel engine injector.* Transactions Journal of Engines, SAE paper 980811, SAE Transactions, 1998. **107**(3).

[5] Roth, H., M. Gavaises and C. Arcoumanis, *Cavitation Initiation, Its Development and Link with Flow Turbulence in Diesel Injector Nozzles.* Transactions Journal of Engines, SAE paper 2002-01-0214, SAE Transactions, 2002. **111**(3): p. 561-580.

[6] Afzal, H., C. Arcoumanis, M. Gavaises and N. Kampanis. *Internal flow in Diesel injector nozzles: modelling and experiments.* in *Proc. 3rd IMeCHE International Seminar on Fuel Injection Systems*. 1999. London, 1-2 Dec.

[7] Gavaises, M. and A. Andriotis. *Vortex Cavitation inside Multi-hole Injectors for large Diesel Engines and its Effect on the Near-nozzle Spray Structure*. in *SAE 2006-01-1114*. 2006.

[8] Andriotis, A., M. Gavaises and C. Arcoumanis, *Vortex flow and Cavitation in Diesel Injector Nozzles.* Journal of Fluid Mechanics, 2008. **10**: p. 195-215.

[9] Gavaises, M., A. Andriotis, D. Papoulias, N. Mitroglou and A. Theodorakakos, *Characterization of string cavitation in large-scale Diesel nozzles with tapered holes.* Physics of Fluids, 2009. **21**: p. 052107.

[10] Arndt, R.E.A., *Cavitation in fluid machinery and hydraulic structures.* Annual Review of Fluid Mechanics, 1981. **13**(1): p. 273-326.

[11] Hsiao, C.T. and L.L. Pauley, *Numerical study of the steady-state tip vortex flow over a finite-span hydrofoil.* Journal of fluids engineering, 1998. **120**: p. 345.

[12] Arndt, R.E.A., *Cavitation in vortical flows.* Annual Review of Fluid Mechanics, 2002. **34**(1): p. 143-175.

[13] Hsiao, C.T. and G.L. Chahine, *Numerical study of cavitation inception due to vortex/vortex interaction in a ducted propulsor.* Journal of Ship Research, 2008. **52**(2): p. 114-123.

[14] Nouri, J.M., N. Mitroglou, Y. Yan and C. Arcoumanis, *Internal Flow and Cavitation in a Multi-Hole Injector for Gasoline Direct-Injection Engines.* SAE SP, 2007-01-1405, 2007. **2084**: p. 23.

[15] Gavaises, M., *Flow in valve covered orifice nozzles with cylindrical and tapered holes and link to cavitation erosion and engine exhaust emissions.* International Journal of Engine Research, 2008. **9**(6): p. 435-447.

[16] Gavaises, M., D. Papoulias, E. Giannadakis, A. Andriotis, N. Mitroglou, and A. Theodorakakos, *Comparison of cavitation formation and development in Diesel VCO nozzles with cylindrical and converging tapered holes*, in *THIESEL 2008*. 2008: Valencia, Spain, 8-10 Sept, 2008.

[17] Andriotis, A., M. Spathopoulou and M. Gavaises. *Effect of nozzle flow and cavitation structures on spray development in low-speed two-stroke Diesel engines*. in *25th CIMAC World Congress on Combustion Engine Technology*. 2007. 21–24 May 2007, Vienna.

[18] Soteriou, C., R. Andrews, N. Torres, M. Smith and R. Kunkulagunta. *Through the diesel nozzle hole–a journey of discovery*. in *ILASS-Europe. 2001*. 2001. September 2-6. Zurich, Switzerland.

[19] Blessing, M., G. Konig, C. Kruger, U. Michels and V. Schwarz. *Analysis of flow and cavitation phenomena in diesel injection nozzles and its effects on spray and mixture formation*. 2003: Professional Engineering for the Institution of Mechanical Engineers.

[20] Soteriou, C., M. Lambert, S. Zuelch and D. Passerel. *The flow characteristics of high efficiency Diesel nozzles with enhanced geometry holes*. in *THIESEL International Conference on Thermo- and Fluid Dynamic Processes in Diesel Engines*. 2006. Valencia, Spain.

[21] Soteriou, C.C.E., M. Smith and R.J. Andrews. *Cavitation Hydraulic Flip and Atomization in Direct Injection Diesel Sprays, IMechE*. in *IMechE*. 1993. London.

[22] He, L. and F. Ruiz, *Effect of cavitation on flow and turbulence in plain orifices for high-speed atomization.* Atomization and Sprays, 1995. **5**(6): p. 569-584.

[23] Soteriou, C., R. Andrews and M. Smith, *Direct injection diesel sprays and the effect of cavitation and hydraulic flip on atomization.* SAE technical paper, 1995. **950080**.

[24] Kim, J.H., K. Nishida and H. Hiroyasu, *Characteristics of the internal flow in a diesel injection nozzle.* International Journal of Fluid Mechanics Research, 1997. **24**(1-3).

[25] Soteriou, C., M. Smith and R. Andrews. *Diesel injection: laser light sheet illumination of the development of cavitation in orifices*. in *IMechE Paper C529/018/98*. 1998.

[26] Giannadakis, E., D. Papoulias, M. Gavaises, C. Arcoumanis, C. Soteriou, and W. Tang, *Evaluation of the predictive capability of diesel nozzle cavitation models.* SAE Paper 2007-01-0245, 2007.

[27] Miranda, R., H. Chaves, U. Martin and F. Obermeier, *Cavitation in a Transparent Real Size VCO Injection Nozzle.* Proceedings of ICLASS, Sorrento Italy, 2003.

[28] Arcoumanis, C., M. Gavaises, H. Flora and H. Roth, *Visualisation of Cavitation in Diesel Engine Injectors.* Mec.Ind., 2001. **2**: p. 375-381.

[29] Roth, H., E. Giannadakis, M. Gavaises, C. Arcoumanis, K. Omae, I. Sakata, M. Nakamura, and H. Yanagihara, *Effect of Multi-Injection Strategy on Cavitation Development in Diesel Injector Nozzle Holes.* Transactions Journal of Engines, SAE paper 2005-01-1237, 2005. **114-3**: p. 1029-1045.

[30] Giannadakis, E., , *Modelling of Cavitation in Automotive Fuel Injector Nozzles* in *Mechanical Engineering, Thermofluids Section*. 2005, Imperial College, University of London: London.

[31] Schmidt, D., C.J. Rutland and M.L. Corradini, *A FULLY COMPRESSIBLE, TWO-DIMENSIONAL MODEL OF SMALL, HIGH-SPEED, CAVITATING NOZZLES.* Atomisation and Sprays, 1999. **9**(3): p. 255-276.

[32] Singhal, A.K., M.M. Athavale, H. Li and Y. Jiang, *Mathematical basis and validation of the full cavitation model.* Journal of fluids engineering, 2002. **124**: p. 617.

[33] Graham, M., N. Keeler and J. Kewley. *Ultra-high pressure common rail systems*. in *Injection Systems for IC Engines*. 2009. IMechE, London, UK.

[34] Giannadakis, E., M. Gavaises and A. Theodorakakos. *The Influence of Variable Fuel Properties in High-Pressure Diesel Injectors*. in *SAE 2009-01-0832*. 2009.

[35] Gavaises, M., D. Papoulias, A. Andriotis, E. Giannadakis and A. Theodorakakos. *Link Between Cavitation Development and Erosion Damage in Diesel Injector Nozzles*. in *SAE 2007-01-0246*. 2007.

[36] Liverani, L., C. Arcoumanis, H. Yanagihara, I. Sakata and K. Omae. *Imaging of the Flow and Cavitation Formation in a Transparent Real-Size Six-Hole Nozzle under Realistic Conditions*. in *COMODIA, Paper SC14*. 2008. Hokkaido University, Japan.

[37] Liverani, L., *Cavitation in Real-Size Diesel Injector Nozzles*, in *School of Engineering and Mathematical Sciences*. 2010, City University London: London.

[38] Gavaises, M., A. Andriotis and C. Arcoumanis, *Complex cavitation structures in Diesel fuel injector nozzles*, in *IMechE conference on "Injection Systems for IC Engines"* 2009: London, 13-14 May, 2009.